BMC Plant Biology

RESEARCH Open Access

Genome-wide characterization of nitric oxide-induced NBS-LRR genes from *Arabidopsis thaliana* and their association in monocots and dicots

Ashim Kumar Das[1], Adil Hussain[1,2*], Nusrat Jahan Methela[1], Da-Sol Lee[1], Geum-Jin Lee[1], Youn-Ji Woo[1] and Byung-Wook Yun[1*]

Abstract

Background Nitric oxide (NO) is pivotal in regulating the activity of NBS-LRR specific *R* genes, crucial components of the plant's immune system. It is noteworthy that previous research has not included a genome-wide analysis of NO-responsive *NBS-LRR* genes in plants.

Results The current study examined 29 NO-induced *NBS-LRR* genes from *Arabidopsis thaliana*, along with two monocots (rice and maize) and two dicots (soybean and tomato) using genome-wide analysis tools. These *NBS-LRR* genes were subjected to comprehensive characterization, including analysis of their physio-chemical properties, phylogenetic relationships, domain and motif identification, exon/intron structures, *cis*-elements, protein-protein interactions, prediction of S-Nitrosylation sites, and comparison of transcriptomic and qRT-PCR data. Results showed the diverse distribution of *NBS-LRR* genes across chromosomes, and variations in amino acid number, exons/introns, molecular weight, and theoretical isoelectric point, and they were found in various cellular locations like the plasma membrane, cytoplasm, and nucleus. These genes predominantly harbor the NB-ARC superfamily, LRR, LRR_8, and TIR domains, as also confirmed by motif analysis. Additionally, they feature species-specific PLN00113 superfamily and RX-CC_like domain in dicots and monocots, respectively, both responsive to defense against pathogen attacks. The NO-induced *NBS-LRR* genes of Arabidopsis reveal the presence of *cis*-elements responsive to phytohormones, light, stress, and growth, suggesting a wide range of responses mediated by NO. Protein-protein interactions, coupled with the prediction of S-Nitrosylation sites, offer valuable insights into the regulatory role of NO at the protein level within each respective species.

Conclusion These above findings aimed to provide a thorough understanding of the impact of NO on *NBS-LRR* genes and their relationships with key plant species.

Keywords *Arabidopsis thaliana*, Nitric oxide, NBS-LRR, Plant immunity, Genome-wide study

*Correspondence:
Adil Hussain
adilhussain@awkum.edu.pk
Byung-Wook Yun
bwyun@knu.ac.kr

[1]Department of Applied Biosciences, College of Agriculture and Life Sciences, Kyungpook National University, Daegu 41566, South Korea
[2]Department of Agriculture, Abdul Wali Khan University Mardan, Khyber Pakhtunkhwa, Pakistan

Introduction

High temperatures and excessive moisture create favorable conditions for pathogens to assail plants, posing a significant threat to global crop production. Nonetheless, plants have developed complex strategies over time to defend against pathogens. This involves the recognition of pathogen-associated molecular patterns (PAMPs) by the plants through PAMP recognition receptors (PRRs), ultimately leading to the induction of PAMP-triggered immunity (PTI) [1]. However, some pathogens can overcome PTI by delivering an armada of effector molecules that increase their pathogenicity and virulence, thereby causing effector-triggered susceptibility (ETS). On the other hand, resistant plants can recognize pathogen effectors via resistance (*R*) gene products resulting in effector-triggered immunity (ETI) [1]. After the identification of the first *R* gene, *Hm1*, in maize in 1992, more than 300 *R* genes from various plant species have been described, with 60% belonging to the large family of nucleotide-binding sites and leucine-rich repeats (NBS-LRR) gene family [2, 3]. These *NBS-LRR* genes encode proteins featuring a diverse amino (N)-terminal domain, a central nucleotide-binding site (NBS), and a leucine-rich repeats (LRR) domain at the carboxy (C)-terminal [4]. The NBS domain, comprising approximately 300 amino acids with specific motifs arranged in a defined order, plays a crucial role in binding and hydrolyzing ATP and GTP during the establishment of plant disease resistance; conversely, the LRR motif within the NBS-LRR protein is responsible for recognizing virulence factors (effectors) released by the pathogens [4–6]. NBS-LRR proteins can recognize a diverse range of effectors released by phytopathogens including bacteria, fungi, viruses, and even insects [7].

The *R* genes encoding the *NBS-LRR* family proteins are further classified into two main groups. The first group consists of proteins with the TOLL/interleukin-1 receptor (TIR) domain, and is designated as the TNL group of proteins (representing TIR-NBS-LRR proteins). The second protein group is characterized by the presence of a coiled-coil (CC) domain at the N-terminal and designated as the CC-NBS-LRR group of proteins [1, 4]. Additionally, a small group of non-TNL genes with RPW8 (resistance to powdery mildew8) domains have also been identified [8, 9], where RPW8-NBS-LRR (RNL) genes have been recognized as parallel to the CNL genes [10].

Recent advancements in plant genome sequencing technologies have accelerated the genome-wide discovery, identification, and analysis of *NBS-LRR* genes in many species, for example, *Arabidopsis thaliana* (189 *NBS-LRR* genes) [6]; *Actinidia chinensis* (100) [11]; *Akebia trifoliata* (73) [12]; *Cicer arietinum* (121) [13]; *Citrus sinensis* (111) [14]; *Cucumis sativus* (33) [15]; *Lagenaria siceraria* (84) [16]; *Dioscorea rotundata* (167) [17]; *Populus trichocarpa* (402) [18]; *Triticum aestivum* (2151) [19], *Vitis vinifera* (352) [20] and other plant species. Overexpressing the grape *VaRGA1* and soybean *GMKR3* TNL genes significantly enhanced disease resistance [21, 22]; whereas, the down-regulation of the cotton *NBS-LRR* gene *GbaNA1* compromised the defense against *Verticillium dahliae* [23]. These studies emphasize the widespread distribution of *NBS-LRR* genes throughout the plant kingdom and can play a crucial role in developing novel resistance traits. Comparative analysis not only enhances our understanding of evolutionary processes and pathogen-resistance mechanisms across species but also reveals insights into discovering new R genes.

An oxidative burst is characterized by the rapid generation of reactive oxygen species (ROS) soon after infection followed by the activation of numerous plant genes crucial for cellular defense. However, this ROS burst alone proves insufficient for a robust disease-resistance response [24, 25]. Delledonne, et al. [26] reported that nitric oxide (NO) regulates plant immunity by facilitating the induction of hypersensitive response (HR) cell death. Subsequent findings revealed an increase in NO levels following *R*-gene-dependent pathogen recognition triggered by the production of the immune activator salicylic acid (SA) and immune-response genes [27]. NO covalently binds to specific reactive cysteine (Cys) thiols in proteins, forming S-nitrosothiols (SNOs). The nitrosative burst plays a crucial role in activating a distinct set of NO-responsive proteins, via NO signaling. This signaling cascade regulates the synthesis of SA [28], triggers HR [29], and, in certain cases, results in the closure of stomata [30]. Additionally, the conjugation of pathogens and PAMPs displayed an influx of extracellular Ca^{2+} influencing pathways upstream of endogenous NO production [31, 32]. The nitrate reductases gene, *NIA1* and *NIA2*, play essential roles in producing NO during immune responses and are closely linked to NO synthesis [33–36]. When SA was applied to mutant lines *nia1*, *nia2*, and *nia1nia2*, a notable reduction in NO production was observed compared to WT. Moreover, inoculating these mutant lines with the pathogen *Pseudomonas syringae* pv. *maculicola* resulted in reduced NO response [34, 37]. S-nitrosoglutathione (GSNO) reductase is the main regulator of the dynamic processes of S-nitrosylation and denitrosylation within cells [32, 38]. The connection between GSNOR activity and immune function was initially uncovered with a loss-of-function mutation in *A. thaliana*, *atgsnor1-3* led to a significant rise in cellular SNO levels [39]. The *gsnor1-3* line demonstrates the loss of various modes of plant immunity, including non-host resistance, basal defense, and R-gene-mediated protection [40] indicating the importance of NO in regulating plant immunity at the molecular level. Afterward, the loss of *GSNOR* function in plants has been shown to

regulate multiple modes of disease resistance as well as overall plant development [41, 42].

Therefore, the nitric oxide (NO)-induced *NBS-LRR* transcripts of *Arabidopsis thaliana* present opportunities for comprehensive characterization through genome-wide analysis, and their potential relationship with the non-model species as homologs of the Arabidopsis NO-responsive *NBS-LRR* genes in monocots (*Oryza sativa* and *Zea mays*) and dicots (*Glycine max* and *Solanum lycopersicum*). It is worth noting that none of the prior studies report a genome-wide analysis of NO-responsive *NBS-LRR* genes in plants. This study identified twenty-nine NO-induced *NBS-LRR* transcripts through transcriptome analysis of Arabidopsis accession Col-0 leaf samples at the rosette stage after 6 h of infiltration with 1mM S-nitrosocysteine (CysNO). Additionally, twenty-seven genes from monocots and dicots were included for further investigation, encompassing phylogenetic analysis, gene structure, *cis*-elements, domain and motif identification, protein-protein interaction, S-Nitrosylation sites, and finally validation of transcriptomic and q-RT PCR results.

Results

Identification of physio-chemical attributes of NBS-LRR genes

Twenty-nine (29) *NBS-LRR* genes were identified as responsive to nitric oxide (NO), with 17 genes displaying upregulation and 12 genes exhibiting downregulation following NO infiltration into Arabidopsis leaves. To conduct a comparative analysis of these NO-induced *NBS-LRR* genes, we specifically chose *NBS-LRR* genes from widely cultivated monocots (*O. sativa* and *Z. mays*) and dicots (*G. max* and *S. lycopersicum*) (Table 1). We found the Arabidopsis genes were mostly distributed on all the chromosomes, but they were especially abundant on AtChr1 and AtChr5; whereas, other species including rice (OsChr1, OsChr6, and OsChr12), maize (ZmChr2, ZmChr4, ZmChr5, ZmChr8, and ZmChr10), soybean (GmChr3, GmChr6, GmChr13, GmChr15, GmChr16, GmChr18, and GmChr19), and tomato (SlChr5, SlChr7, and SlChr12) were also well scattered on the different chromosomes. In detail, chromosomal location and their distribution are shown in Table 1. For the *NBS-LRR* genes of Arabidopsis, the CDS length was between 519 and 5235 bp; moreover, rice, maize, soybean, and tomato genes spanned 1482–4437, 2592–3336, 1911–3678, and 588–4275 bp, respectively. The longest protein was encoded by *AT1G69550.1* (1401 aa) in Arabidopsis, *LOC_Os06g49390.1* (1479 aa) in rice, *Zm00001eb349360_T002* (1112 aa) in maize, *Glyma.03g037300.2* (1226 aa) in soybean, and *Solyc12g097000.2.1* (196 aa) in tomato. Conversely, the shortest protein was encoded by the gene *AT1G57630.1* (173 aa) in Arabidopsis, *LOC_Os12g32670.1* (494 aa) in rice, *Zm00001eb197290_T001* (864 aa) in maize, *Glyma.16g118600.2* (584 aa) in soybean, and *Solyc05g006620.2.1* (1425 aa) in tomato (Table 1). In addition, the molecular weight displayed noteworthy variation, ranging from 19.412 to 196.906, 55.29434-166.47254, 97.16231–124.4716, 66.45707–139.6676, and 22.25826-159.72534 kDa in Arabidopsis, rice, maize, soybean, and tomato, respectively. The proteins encoded by NBS-LRR-related genes in tomato were consistently acidic, characterized by their isoelectric points below 7. On the other hand, while over half of the proteins encoded by NBS-LRR-related genes in Arabidopsis were also acidic, those from rice, maize, and soybean were predominantly alkaline, featuring higher isoelectric point values (Table 1). ExPASy database analysis showed that most *NBS-LRR* proteins in Arabidopsis, rice, maize, soybean, and tomato were hydrophilic (GRAVY < 0), except for one Arabidopsis gene (*AT1G69550.1*). The Arabidopsis NBS-LRR proteins were predicted to be localized in the plasma membrane, cytoplasm, chloroplast, and nucleus, those of the monocots and dicots were predominantly localized only in the cytoplasm, as predicted by the subCELlular Localization predictor CELLO v.2.5 (Table 1).

Phylogenetic relationship and structural domain analysis

Using the Maximum Likelihood method, a phylogenetic tree was created to analyze the evolutionary relationships among *NBS-LRR* genes in Arabidopsis (AT), rice (LOC), maize (Zm), soybean (Glyma), and tomato (Solyc). The genes were categorized into groups represented by different colors (Fig. 1A; Supplementary Table 1). The purple clade, composed mostly of Arabidopsis genes, displays many closely related genes, highlighting high similarity within this species. The red clade, which includes soybean, tomato, and Arabidopsis genes, forms a distinct cluster, suggesting unique evolutionary paths or functions for these species. The blue clade, containing maize genes, shows significant clustering, pointing to species-specific evolutionary pressures or constraints. Similar to soybean and tomato, rice genes exhibit diverse branching patterns, suggesting varied evolutionary histories or adaptation strategies. The phylogenetic tree not only shows the similarities and differences between the gene sequences but also gives useful information about how a set of genes evolves in different plant species and how they are related to each other.

Subsequently, conserved domains were identified with the help of the NCBI Conserved Domain Database (https://www.ncbi.nlm.nih.gov/Structure/cdd/wrpsb.cgi) and TBtools. A total of 14 domains were found in all species, including RX-CC-like, NB-ARC superfamily, LRR superfamily, PLN03210 superfamily, TIR, C-JID, Rx-N, C-JID superfamily, PPP1R42 superfamily, NB-ARC,

Table 1 List of genes and the physio-chemical attributes of NBS-LRR genes in *A. Thaliana*, *O. sativa*, *Z. mays*, *G. Max*, and *S. Lycopersicum*

Transcript No.	Transcript ID	Chr	Location Start-End	Strand	CDS (bp)	Protein length (aa)	Protein molecular weight (kDa)	Isoelectric point (pI)	GRAVY	Subcellular localization
01	AT1G17610.1	1	6,054,921–6,058,357	Forward	1263	421	47.756	5.89	-0.157	Cytoplasmic
02	AT1G31540.2	1	11,288,377–11,293,799	Reverse	3486	1162	133.493	5.48	-0.25	Nuclear
03	AT1G56540.1	1	21,181,584–21,185,495	Forward	3291	1097	125.009	6.57	-0.207	Plasma membrane
04	AT1G57630.1	1	21,345,444–21,346,157	Forward	519	173	19.412	7.69	-0.165	Chloroplast
05	AT1G57650.1	1	21,351,165–21,354,311	Forward	2130	710	82.042	5.5	-0.182	Nuclear
06	AT1G63750.3	1	23,650,839–23,655,453	Forward	3396	1132	128.069	5.53	-0.333	Nuclear
07	AT1G66090.1	1	24,602,032–24,604,763	Forward	1290	430	48.023	7.22	-0.211	Nuclear; Plasma membrane
08	AT1G69550.1	1	26,148,020–26,153,600	Reverse	4203	1401	155.201	5.76	0.051	Plasma membrane; Nuclear
09	AT1G72890.2	1	27,429,915–27,432,003	Forward	1464	488	56.697	9.56	-0.276	Plasma membrane; Mitochondrial; Nuclear
10	AT2G20142.1	2	8,695,373–8,696,643	Forward	942	314	36.196	8.31	-0.035	Plasma membrane
11	AT3G04220.3	3	1,108,724–1,112,437	Reverse	2691	897	102.043	6.21	-0.276	Nuclear
12	AT3G25510.1	3	9,263,794–9,268,972	Reverse	3246	1326	121.111	5.7	-0.02	Nuclear
13	AT3G44400.1	3	16,044,661–16,049,803	Reverse	3024	1008	115.784	7.49	-0.241	Nuclear
14	AT3G44670.1	3	16,216,805–16,221,722	Forward	3660	1220	139.09	6.33	-0.243	Nuclear
15	AT4G14370.2	4	8,279,633–8,283,535	Reverse	3156	1052	120.185	6.37	-0.332	Nuclear
16	AT4G19520.1	4	10,639,268–10,647,280	Reverse	5235	1745	196.906	8.64	-0.181	Nuclear
17	AT5G17880.1	5	5,908,833–5,913,317	Reverse	3594	1198	135.859	8.12	-0.388	Nuclear
18	AT5G22690.2	5	7,541,071–7,545,256	Forward	3033	1011	115.220	8.11	-0.195	Nuclear
19	AT5G40060.1	5	16,034,441–16,039,096	Forward	2907	968	109.424	8.18	-0.147	Nuclear
20	AT5G40910.1	5	16,394,461–16,400,489	Forward	3315	1105	124.314	6.77	-0.066	Plasma membrane; Nuclear
21	AT5G41550.1	5	16,617,231–16,620,824	Reverse	3258	1086	122.064	7.33	-0.183	Nuclear
22	AT5G41740.2	5	16,688,625–16,693,119	Forward	3345	1115	125.492	8.44	-0.184	Nuclear
23	AT5G44910.1	5	18,137,348–18,138,757	forward	726	242	27.518	6.14	-0.17	Plasma membrane
24	AT5G46260.1	5	18,758,698–18,763,503	reverse	3618	1206	137.472	7.71	-0.266	Nuclear
25	AT5G46270.4	5	18,763,971–18,769,090	reverse	3438	1146	130.415	5.6	-0.176	Nuclear
26	AT5G46510.1	5	18,860,233–18,867,015	forward	4062	1354	153.544	5.09	-0.296	Nuclear
27	AT5G43740.1	5	17,564,696–17,569,148	forward	2589	863	98.472	5.64	-0.079	Cytoplasmic
28	AT5G63020.1	5	25,283,062–25,286,121	reverse	2667	889	101.801	6.18	-0.135	Cytoplasmic; Nuclear
29	AT5G66910.1	5	26,718,129–26,721,377	reverse	2448	816	92.93	5.41	-0.095	Cytoplasmic; Nuclear
30	LOC_Os01g16370.1	1	9,293,170–9,299,788	forward	2331	777	88.25878	9.03	-0.113	Cytoplasmic
31	LOC_Os06g05359.1	6	2,410,175–2,418,568	forward	3081	1027	117.68518	8.35	-0.304	Cytoplasmic
32	LOC_Os06g06380.1	6	2,973,520–2,979,496	reverse	2865	955	108.01102	8.25	-0.087	Cytoplasmic
33	LOC_Os06g41670.1	6	24,954,261–24,959,578	reverse	1740	580	66.4109	8.52	-0.188	Cytoplasmic
34	LOC_Os06g49390.1	6	29,926,769–29,931,821	reverse	4437	1479	166.47254	6.32	-0.204	Cytoplasmic
35	LOC_Os12g32670.1	12	19,716,107–19,719,992	reverse	1482	494	55.29434	6.68	-0.259	Cytoplasmic
36	Zm00001eb115030_T001	2	235,315,765–235,322,044	reverse	3141	1047	116.09234	8.67	-0.248	Cytoplasmic
37	Zm00001eb197290_T001	4	195,390,851–195,393,586	reverse	2592	864	97.16231	8.04	-0.159	Cytoplasmic
38	Zm00001eb226710_T001	5	57,365,615–57,387,844	reverse	2700	900	103.00206	6.84	-0.091	Cytoplasmic
39	Zm00001eb349360_T002	8	106,610,582–106,614,710	reverse	3336	1112	124.4716	8.92	-0.214	Cytoplasmic
40	Zm00001eb405270_T001	10	1,566,941–1,573,505	reverse	3120	1040	119.13999	7.23	-0.263	Cytoplasmic
41	Glyma.03g037100.2	3	4,541,759–4,546,288	forward	3663	1221	138.66895	5.87	-0.204	Cytoplasmic
42	Glyma.03g037300.2	3	4,566,741–4,573,890	forward	3678	1226	139.6676	6.37	-0.201	Cytoplasmic

Table 1 (continued)

Transcript No.	Transcript ID	Chr	Location Start-End	Strand	CDS (bp)	Protein length (aa)	Protein molecular weight (kDa)	Isoelectric point (pI)	GRAVY	Subcellular localization
43	Glyma.03g088100.2	3	26,147,637–26,152,559	forward	2778	926	105.11203	6.29	-0.189	Cytoplasmic
44	Glyma.06g259800.2	6	45,555,048–45,558,566	reverse	3609	860	99.50453	5.01	-0.39	Cytoplasmic
45	Glyma.06g267300.2	6	45,555,048–45,558,566	forward	1911	637	72.65473	8.4	-0.323	Cytoplasmic
46	Glyma.13g184800.2	13	29,858,000–29,863,047	reverse	3198	1066	121.57487	7.87	-0.266	Cytoplasmic
47	Glyma.15g168500.2	15	15,007,753–15,012,598	reverse	2763	921	105.43098	6.83	-0.236	Cytoplasmic
48	Glyma.16g118600.2	16	26,442,194–26,445,922	forward	2394	584	66.45707	8.05	-0.173	Cytoplasmic
49	Glyma.18g287100.2	18	56,710,302–56,713,686	reverse	2286	762	87.22922	8.9	-0.258	Cytoplasmic
50	Glyma.19g134200.1	19	39,523,361–39,525,814	reverse	2220	740	84.3507	7.57	-0.083	Cytoplasmic
51	Solyc05g006620.2.1	5	1,267,541–1,277,499	reverse	4275	1425	159.72534	6.33	-0.115	Cytoplasmic
52	Solyc05g006630.2.1	5	1,281,454–1,291,211	forward	4098	1366	153.92672	6.12	-0.18	Cytoplasmic
53	Solyc07g052770.2.1	7	61,218,509–61,222,379	forward	2922	974	111.40282	5.78	-0.148	Cytoplasmic
54	Solyc07g052800.2.1	7	61,375,262–61,376,839	forward	1155	385	44.21608	6.36	-0.143	Cytoplasmic
55	Solyc12g097000.2.1	12	65,199,380–65,200,267	reverse	588	196	22.25826	6.17	-0.297	Cytoplasmic
56	Solyc12g097010.1.1	12	65,201,249–65,204,709	reverse	2298	765	88.26968	5.53	-0.225	Cytoplasmic

LRR-8, PLN00113 superfamily, LRR, and RPW8 superfamily (Fig. 1B; Supplementary Table 2). The *NBS-LRR* genes from all the species under study were categorized according to their number of domains, wherein the largest number of domains were found in *AT4G19520.1* (two PLN00113 superfamily, one each from the LRR superfamily, and TIR domains). Except *AT5G63020.1*, *AT5G43740.1*, *AT2G20142.1*, and *AT5G44910.1*, the majority of NO-induced *NBS-LRR* genes in Arabidopsis primarily possessed the PLN00113 superfamily domain. Conversely, genes lacking the PLN00113 superfamily domain typically contained domains such as NB-ARC superfamily, LRR, LRR-8, and TIR domains (Fig. 1B). Apart from the soybean gene *Glyma.18g287100.2*, all other genes retain the PLN00113 superfamily domain in addition to RX-CC-like, NB-ARC superfamily, Rx-N, and PPP1R42 superfamily domains. However, *NBS-LRR* genes in rice and maize lack the PLN00113 superfamily domain and primarily contain RX-CC-like, NB-ARC superfamily, LRR superfamily, and Rx-N domains (Fig. 1B). Tomato genes exhibit conserved domains, including the PLN00113 superfamily, PLN00113 superfamily, C-JID, and TIR. Comparative domain analysis among NO-induced Arabidopsis genes with the homologs of the Arabidopsis NO-responsive genes of monocots (rice and maize) and dicots (soybean and tomato) revealed the shared and conserved history of the NBS-LRR domain along with other domains in these plant species.

Gene structure and putative *cis*-regulatory element analysis

A total of 56 *NBS-LRR* genes were identified across *A. thaliana*, *O. sativa*, *Z. mays*, *G. max*, and *S. lycopersicum*, each displaying distinct exon and intron patterns as determined by the Gene Structure Display Server 2.0 (Fig. 2A). Based on the number of exons present, these genes were categorized using different colors. Approximately 5–8 exons were observed in 15 genes of Arabidopsis, as well as in two dicots (soybean and tomato), while all genes from monocots (rice and maize) had up to a maximum of 3 exons. Furthermore, certain *NBS-LRR* genes in Arabidopsis (*AT5G43740.1*, *AT1G7610.1*, and *AT1G57630.1*), rice (*LOC_Os06g41670.1* and *LOC_Os12g32670.1*), soybean (*Glyma.03g037300.2*, *Glyma.03g037100.2*, *Glyma.13g184800.2*, and *Glyma.19g134200.1*) and maize (*Zm00001eb349360_Too2*) had no introns (Fig. 2A).

Additionally, using the PlantCARE database, we evaluated the NBS-LRR genes from A. *thaliana*, *O. sativa*, *Z. mays*, *G. max*, and *S. lycopersicum* for the distribution of *cis*-regulatory elements (CREs) within a 1 kb promoter region of each gene. These CREs were then categorized and summed based on their functions in plant development and their responses to phytohormones, light and different environmental conditions. Detailed information regarding the identified CREs in the corresponding *NBS-LRR* genes is provided in Supplementary Table 3. Analysis revealed that among the 56 *NBS-LRR* genes examined, 23 genes were found to harbor a significant number of CREs, including those responsive to phytohormones, light, stress, and plant growth and development (Fig. 2B). Furthermore, 10 genes from Arabidopsis, 3 from rice, 2 from maize, 6 from soybean, and 2 from tomato contained CREs responsible for regulating plant growth and development (Fig. 2B; red box). Additionally, we observed that all genes contained CREs responsive to light in their promoter sequences, whereas *AT5G22690.2* and *Solyc05g006630.2.1*, carried light-responsive CREs only (Fig. 2B; yellow box). After light-responsive CREs, *NBS-LRR* genes also contained various phytohormone-responsive CREs in their promoter regions. These include

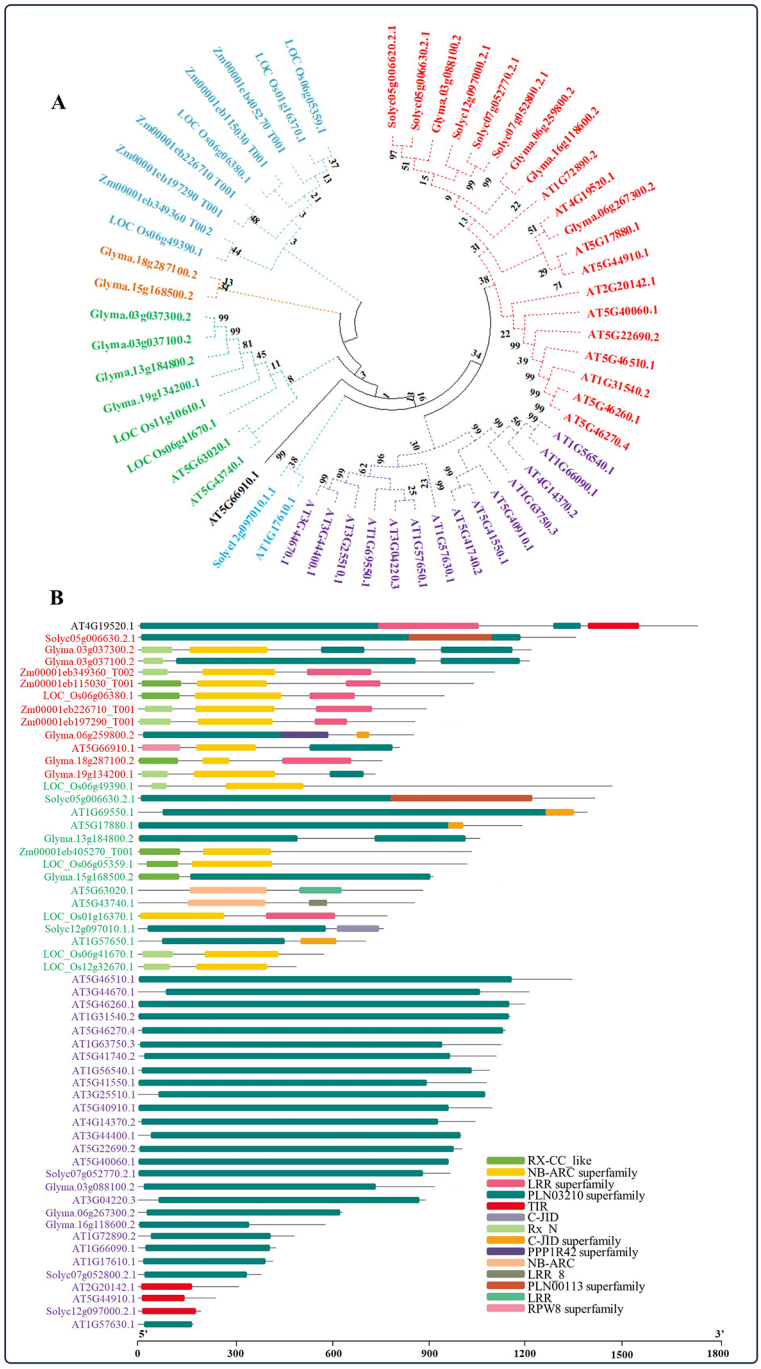

Fig. 1 Phylogenetic analysis and the identification of conserved domains. A Maximum Likelihood phylogenetic tree of *A. thaliana*, *O. sativa*, *Z. mays*, *G. max*, and *S. lycopersicum* NBS-LRR mRNA sequences was created using MEGA X 10.1.8 with 1000 bootstrap replications (**A**). The highly conserved structural domains of NBS-LRR proteins from *A. thaliana*, *O. sativa*, *Z. mays*, *G. max*, and *S. lycopersicum* were mined through the NCBI CDD and visualized by TBtools-II v2.102 that are shown as colored boxes (**B**). The scale bar represents the sequence length in base pairs of proteins used for the analysis (**B**). The respective genes are color-coded based on the number of domains (**B**)

elements responsive to auxin, abscisic acid, salicylic acid, gibberellic acid, and methyl jasmonate (Fig. 2B; green box and Supplementary Table 3). The orthologous *NBS-LRR* genes identified in *A. thaliana*, *O. sativa*, *Z. mays*, *G. max*, and *S. lycopersicum* exhibit shared functional CREs, despite variations in both the types and quantities of CREs present. The unique functions of these CREs in *NBS-LRR* genes, such as involvement in developmental processes, hormone responses, and responses to abiotic

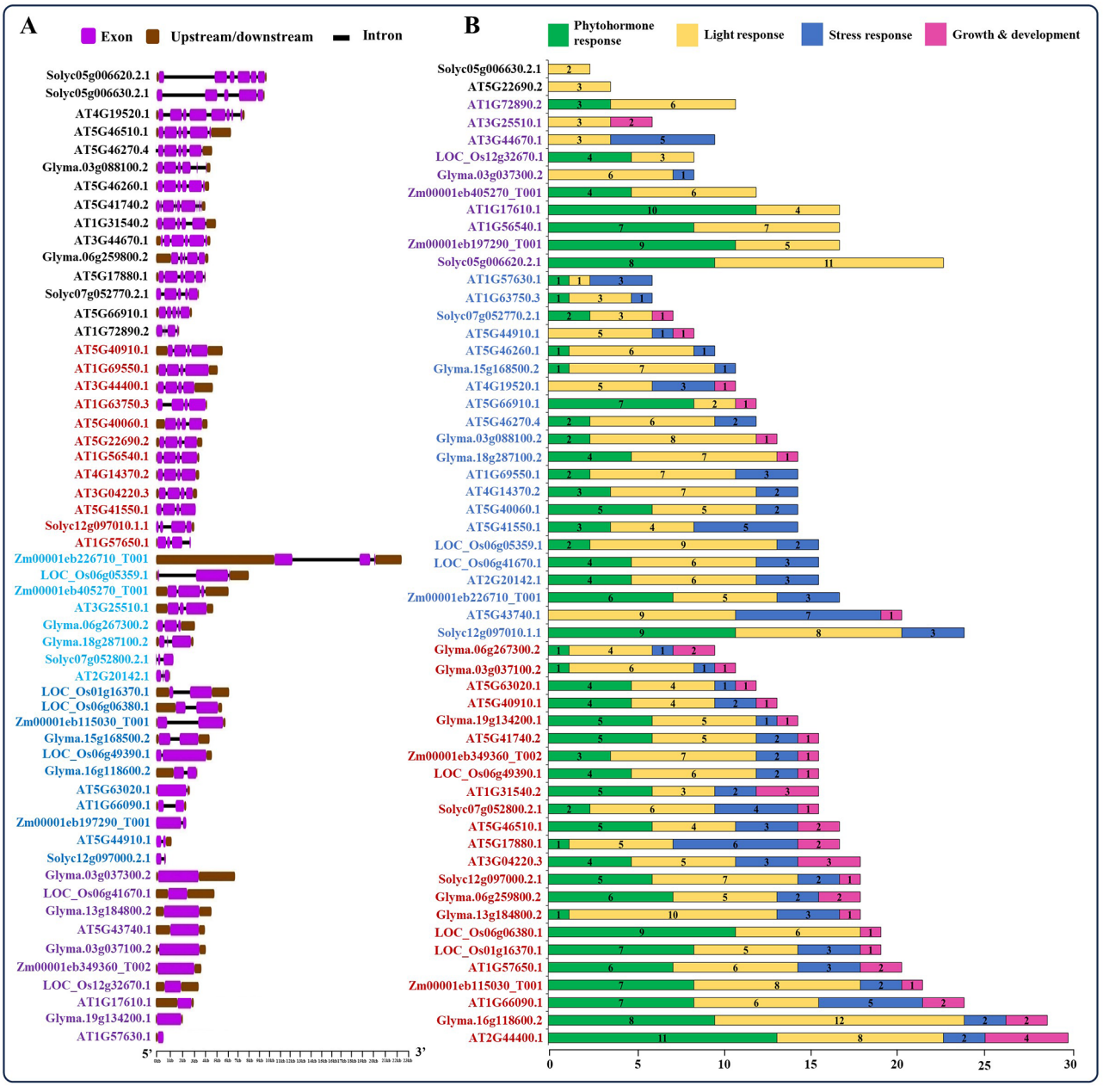

Fig. 2 Gene structure and cis-regulatory elements. The gene structure of *NBS-LRR* genes from *A. thaliana*, *O. sativa*, *Z. mays*, *G. max*, and *S. lycopersicum* with the number, size, and location of introns and exons (**A**). The gene structure was analyzed using Gene Structure Display Server 2.0. Introns and exons are represented by black lines and purple boxes, respectively. The lengths of introns and exons for each gene are displayed proportionally. The color-groups are based on the number of exons of the respective genes (**A**). The distribution of *cis*-regulatory elements (CREs) within the 1 kb promoter region of these NBS-LRR genes was identified using PlantCARE and merged using MS Excel (**B**). Values in the bar graph represent the number of total CREs are involved in phytohormone, light, stress responses or growth and development responses. Several color groups indicate the number of *cis*-elements present in response to phytohormone, light, stress responses or growth and development of the respective genes (**B**)

and biotic stresses, underscore their significance in plant molecular functions.

Conserved motif analysis of *NBS-LRR* genes

The candidate protein sequences underwent motif analysis using the 'MEME' server, revealing the presence of 10 conserved motifs dispersed throughout the protein sequences (Fig. 3). Further validation through Pfam data analysis showed that motifs 1, 6, 7, and 8 were associated with the TIR domain, motif 4 with the NB-ARC domain, and motif 5 with the LRR_3 domain. However, motifs 2, 3, 9, and 10 are not associated with any domains. Additionally, *NBS-LRR* genes from *A. thaliana*, *O. sativa*, *Z. mays*, *G. max*, and *S. lycopersicum*

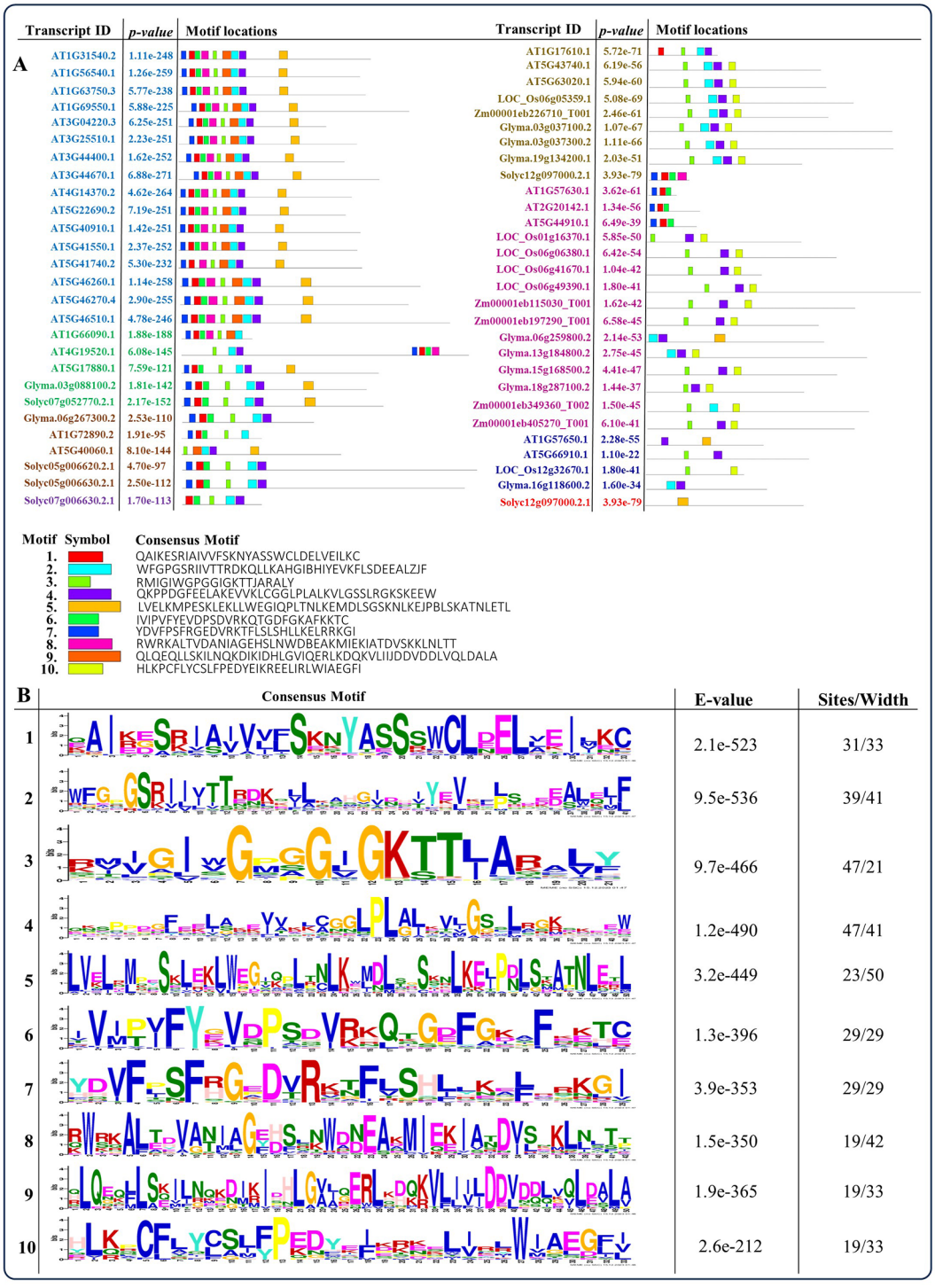

Fig. 3 Identification of motif locations. The MEME tool was employed to conduct conserved motif analysis, resulting in the identification of 10 conserved motifs with sequence IDs, motifs, and logos are provided as part of the analysis (**A**). The respective genes are color-coded based on the presence of a higher number of motifs (**A**). The sequence logos depict ten highly conserved motifs identified in NBS-LRR proteins from *A. thaliana*, *O. sativa*, *Z. mays*, *G. max*, and *S. lycopersicum* (**B**)

were categorized based on their frequency of motifs in the protein sequence and represented with different colors (Fig. 3A). Motif 5 corresponds to the LRR_3 domain, situated at the C-terminus, found in 19 Arabidopsis *NBS-LRR* genes, along with two genes each from soybean and tomato; whereas, *Solyc12g097000.2.1* contained only motif 5. Moreover, in rice and maize, motifs 6 and 10 were notably found at the N- and C-terminal regions,

respectively, with motif numbers ranging from 2 to 4. Similarly, motifs 2 and 4 were commonly detected in soybean genes, mirroring their presence in Arabidopsis genes, although three Arabidopsis genes (*AT1G57630.1*, *AT2G20142.1*, and *AT5G44910.1*) did not exhibit these motifs. Figure 3B displays sequence logos illustrating highly conserved amino acids (minimum 21 to maximum 50). Stacks of letters represent the potential number of amino acids at each position, with the size of the letter indicating their frequency in the sequence. The height of the letter reflects the degree of conservation at that position, with total stack heights providing information on conservation measured in bit score. Higher scores indicate greater conservation, while lower scores signify randomness. The conserved motifs we have identified play a crucial role in elucidating the molecular function of *NBS-LRR* gene family across all species, particularly in the context of plant immunity.

Protein–protein interaction for NBS-LRR genes and predicted S-Nitrosylation active sites

Figure 4A, B, C and D, and 4E represent the predicted protein–protein interaction (PPI) networks for *A. thaliana*, *O. sativa*, *Z. mays*, *G. max*, and *S. lycopersicum*, respectively. In these figures, the majority of identified proteins from each species are categorized as disease resistance proteins associated with the *NBS-LRR* family (Supplementary Table 4). However, in Fig. 4A, the CHS1 protein from Arabidopsis and T8L23.12, known as an ATP-binding protein, were not included in the *NBS-LRR* family. While proteins from Arabidopsis and rice exhibited robust interactions, those from maize, soybean, and tomato showed limited interaction among themselves (Fig. 4).

Additionally, the AlphaFold protein structure revealed differences among the *NBS-LRR* genes within each species and between different species (Supplementary Fig. 1–5). However, we checked the possible S-Nitrosylation sites from NO-induced *NBS-LRR* genes of Arabidopsis; therefore, we chose four TIR-NBS-LRR (*AT4G14370.2*, *AT4G19520.1*, *AT5G40060.1* and *AT5G46270.4*) and two CC-NBS-LRR (*AT5G43740.1* and *AT5G63020.1*) genes based on their highest number of S-Nitrosylation sites identified by the GPS-SNO 1.0 tool. Subsequently, we utilized Pymol to visualize the 3D protein structure, highlighting the respective S-Nitrosylation sites with purple bonds (Fig. 5A; Supplementary Table 5). Similarly, we identified minimum 2 and maximum 6 S-Nitrosylation sites from rice, maize, soybean, and tomato, which were visualized as discussed before (Fig. 5B-E; Supplementary Table 5). Specifically, S-Nitrosylation has the potential to alter the activity of *NBS-LRR* proteins, thereby impacting their capacity to detect pathogens and initiate immune responses [40]. Hence, the identification of specific S-Nitrosylation sites within the listed genes of our studied species presents an opportunity to delve deeper into the molecular mechanisms underlying plant immunity, particularly those involving *NBS-LRR* proteins.

Validation of transcriptional changes of NO-induced NBS-LRR genes by quantitative RT-PCR

Of the 32,535 differentially expressed genes (DEGs), a total of 29 *NBS-LRR* DEGs were recorded in the data set. Of the genes analyzed, 17 were up-regulated, as shown in red in Fig. 6A, while 12 were down-regulated, as shown in blue in the same figure. As a norm, to further validate the transcriptional changes triggered by CysNO treatment, we selected 4 NBS-LRR genes each from up- and down-regulated DEGs, and measured the changes in their transcript accumulation within the first 6 h of infiltration with 1mM CysNO (Fig. 6B). These genes primarily participate in plant defense mechanisms mediated by *NBS-LRR* proteins, along with involvement in other metabolic pathways in plants. A significantly higher correlation (correlation coefficient $R^2=0.97$) was observed in the expression patterns recorded in the qRT-PCR and transcriptomic data. The high correlation coefficient of 0.97 underscores the statistical reliability and comparability of the qRT-PCR results with the RNA-Seq data (Fig. 6).

Discussion

The NBS-LRR (nucleotide-binding site–leucine-rich repeat) family stands out as the predominant and most expansive group of plant R genes (0.2–1.6% in the whole genome), ubiquitous across various plant species [20, 43]. It has been suggested that a resistance protein can optimize its detection capabilities by surveilling or 'guarding' a host protein that is targeted by multiple pathogen effectors [44]. Notably, nitric oxide (NO) contributes to plant defense responses by activating directly or indirectly the defense response R-gene to trigger the production of the immune activator and activated immune-response genes [27, 45, 46]. However, thanks to advancements in DNA sequencing technology, the genomes of many crops have been successfully sequenced. This wealth of genomic data has significantly expedited the discovery and understanding of functional R genes in economically significant plants [47–49], marking the dawn of a new era in molecular breeding [50].

In this investigation, we identified 29 *NBS-LRR* genes induced by NO through transcriptomic analysis of Arabidopsis leaves at the rosette stage. Among these, *AT5G63020.1* and *AT5G66910.1* are recognized as belonging to the CC-NBS-LRR class, while the rest of them are categorized under the TIR-NBS-LRR class family. Additionally, we included two monocots (rice and maize) and two dicots (soybean and tomato) in our

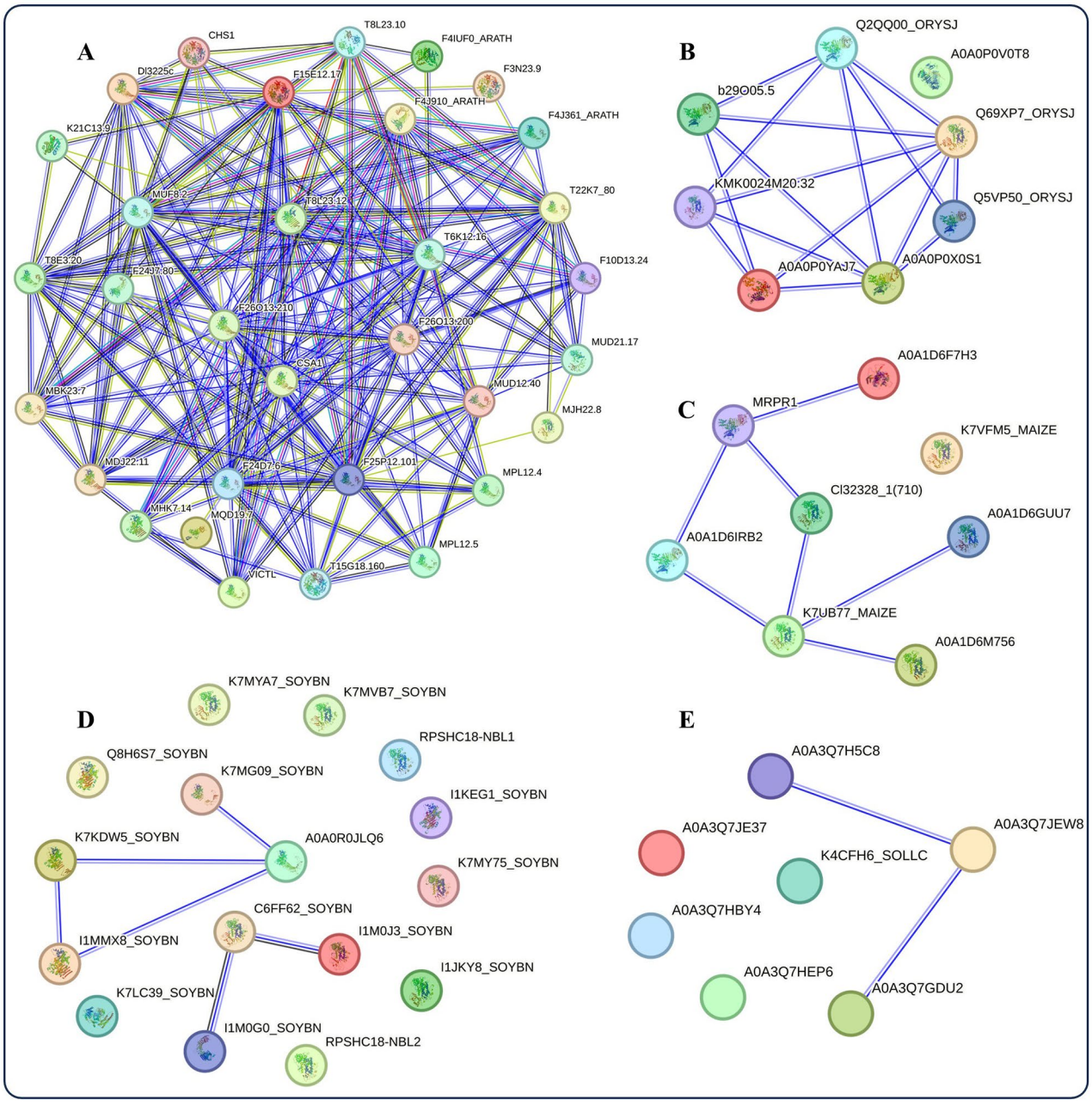

Fig. 4 Protein-protein interaction analysis. The protein-protein interaction (PPIs) analysis of proteins encoded by *NBS-LRR* genes of *A. thaliana* (**A**), *O. sativa* (**B**), *Z. mays* (**C**), *G. max* (**D**), and *S. lycopersicum* (**E**) using STRING v.12. Nodes represent proteins, with empty nodes indicating proteins for which the 3D structures are unknown, and filled nodes indicating proteins with known or predicted 3D structures. Connections between nodes represent interactions between proteins, with different colors indicating different types of interactions

analysis to establish a comparative relationship with the NO-induced *NBS-LRR* genes to understand their structural and functional assessment that has not been previously undertaken. Based on our analysis of the physio-chemical properties of the predicted proteins, we observed the distribution of genes across chromosomes in different plant species shows notable patterns. This chromosomal distribution of Arabidopsis genes may indicate regions of higher gene density or hotspots of genetic activity. Comparatively, in non-model species as homologs of the Arabidopsis NO-responsive proteins present in rice, maize, soybean, and tomato, the gene distribution also spans multiple chromosomes, yet specific chromosomes seem to carry a higher gene load (Table 1). These findings align with previous studies that suggest gene distribution is not uniform across chromosomes but rather exhibits areas of higher gene density [6, 51]. Furthermore, the bioinformatic analyses for the

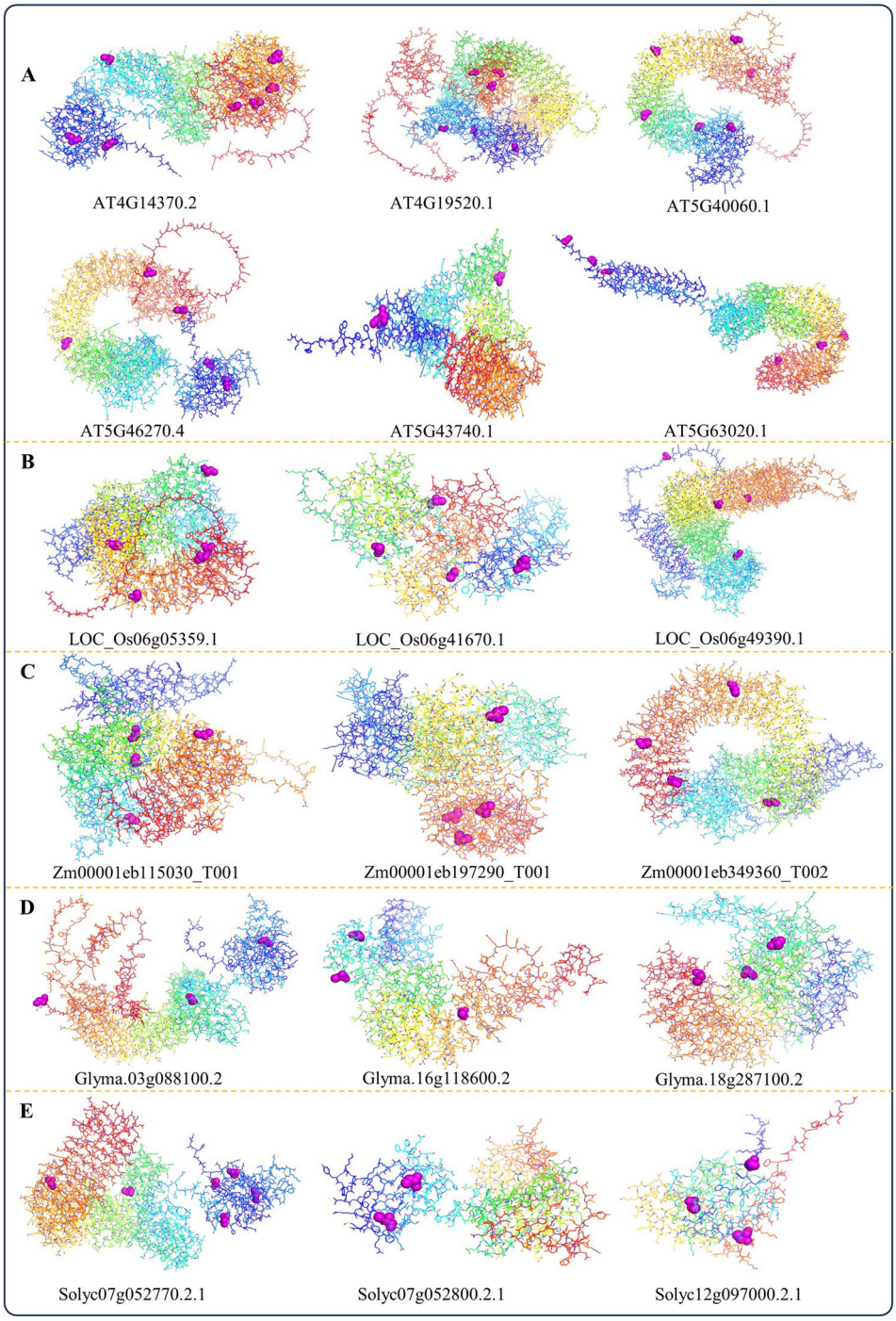

Fig. 5 Prediction of the S-Nitrosylation sites. The putative S-nitrosylation active sites (magenta spheres) within the folding structure of *NBS-LRR* genes of *A. thaliana* (**A**), *O. sativa* (**B**), *Z. mays* (**C**), *G. max* (**D**), and *S. lycopersicum* (**E**) were predicted through using GPS-SNO 1.0 and visualized in PyMol 2.5.5

additional physio-chemical properties such as coding sequence (CDS) length, protein length, molecular weight, isoelectric point (pI), and subcellular localization with genome-wide analyses are comparable with those previously studied on cucumber [15], cabbage [52], and kiwifruit [11]. From our study, most *NBS-LRR* proteins are hydrophilic and predominantly localized in the nucleus and cytoplasm, reflecting their functional roles. Therefore, by leveraging physiochemical findings, researchers can design targeted experiments to unravel the complex roles of *NBS-LRR* genes in plant immunity studies.

The phylogenetic tree of NO-induced *NBS-LRR* genes with monocots and dicots underscores the potential for a distinct evolutionary pattern within the *NBS-LRR* gene

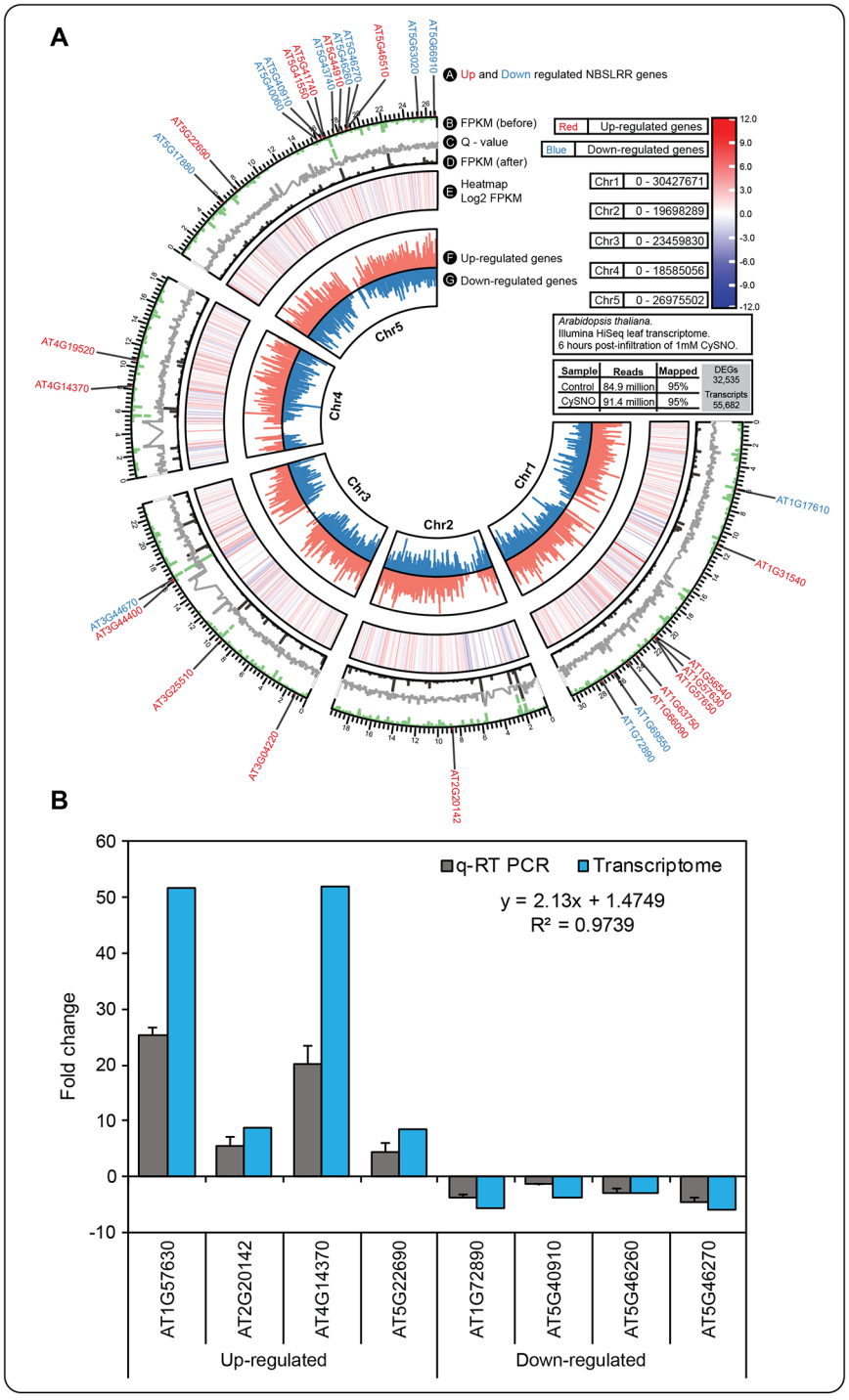

Fig. 6 Expression patterns of NBS-LRR genes in the transcriptomic data and validation via qRT-PCR. CIRCOS plot showing a summary of the CysNO-induced Arabidopsis leaf transcriptomic data (**A**). Of the 32,535 DEGs, a total of 29 *NBS-LRR* genes were recorded with 17 up-regulated (red text) and 12 down-regulated (blue text) genes. Further, a total of 8 genes (4 each from up- and down-regulated DEGs) were selected for validation of their fold change in expression using qRT-PCR analysis (analysis was done by CFX Duet Real-Time PCR System using CFX Maestro 2.3 software) (**B**). These genes are associated with NBS-LRR groups involved in regulating plant immunity. The high correlation coefficient (R) of 0.97 indicates the statistically significant comparability between RNA-Seq and qRT-PCR results (correlation coefficient was done by MS Excel). Error bars represent the standard deviation, with each data point indicating the mean of three replicates

family. Similarly, recent investigations on switchgrass [53] and grapevine [20] revealed the evolutionary conservation of *NBS-LRR* genes. Moreover, our domain analysis revealed that all *NBS-LRR* genes were characterized by NB-ARC superfamily, LRR, LRR_8, and TIR domains, with a notable prevalence of the PLN00113 superfamily domain in dicots, whereas monocots exhibited a higher abundance of the RX-CC_like domain (Fig. 1B). The PLN00113 superfamily and RX-CC_like domains within the *NBS-LRR* gene family interact with pathogen effectors to trigger defense responses. However, they show species specificity, with PLN00113 found in dicots and RX-CC_like in monocots, which is corroborated with our results. Importantly, we identified the C-terminal jelly-roll/Ig-like domain (C-JID) exclusively in the *Solycl12g097010.1.1* gene. To our knowledge, this is the first documented instance of this domain in tomato, discovered through genome-wide analysis. The C-JID is capable of recognizing pathogen effectors by making direct contact with their surface and active-site residues [54]. Similarly, *Glyma.06g259800.2* displayed protein phosphatase 1 regulatory subunit 42 (PPP1R42) domain, also known as leucine-rich repeat-containing protein 67 (LRRC67) or testis leucine-rich repeat (TLRR) protein, which is involved in centrosome separation. It has not been extensively studied in plant immunity. Investigating PPP1R42 in this context could reveal how regulatory subunits affect plant immune responses and pathogen interactions, potentially uncovering new mechanisms of plant defense.

Structural analysis of NO-induced *NBS-LRR* genes in Arabidopsis highlights substantial diversity in exon/intron arrangements, suggesting the evolution of novel specialized functions to better adapt to their environment. While approximately half of the Arabidopsis genes consist of both exons and introns, three of them lack introns entirely (Fig. 2A). Surprisingly, monocots exhibit a range of 0–3 exons, contrasting with the patterns observed in Arabidopsis and dicots. This structural variation arises from three mechanisms: gain/loss of exons/introns, insertion/deletion trials, and exonization/pseudo-exonization processes [55–57]. Consistent with our findings, previous research has also demonstrated variations in the number of exons and introns within *NBS-LRR* proteins in grapevine [20]. The number, position, and length of exons and introns directly impact the 3D folding structure of the proteins, ultimately affecting subsequent protein processing, including post-translational modifications. Promoter *cis*-acting elements are pivotal in regulating gene expression, especially in response to growth, hormonal, and environmental stresses [11, 15, 20]. Analysis of the upstream 1000 bp sequence of NO-induced *NBS-LRR* genes across Arabidopsis, monocots, and dicots reveals a multitude of cis-acting elements linked to phytohormones, light, stress, and plant growth and development (Fig. 2B). Accompanying the disease resistance mechanisms, our selected *NBS-LRR* genes predominantly exhibit light responsiveness, followed by hormonal functions, underscoring their multifaceted roles. Specifically, NO-induced *NBS-LRR* genes of Arabidopsis highlight the presence of ABA and MeJA responsiveness elements, alongside a significant abundance of anaerobic responsiveness elements (Supplementary Table 3), indicating diverse responses mediated by *NBS-LRR* genes through NO.

Analysis of conserved motifs in NO-induced NBS-LRR genes from *A. thaliana*, *O. sativa*, *Z. mays*, *G. max*, *and S. lycopersicum* revealed a total of 10 motifs containing TIR, NB-ARC, and LRR_3 domains (Fig. 3). However, certain motifs within the protein sequence were not recognized as domains through Pfam analysis. This discrepancy may be attributed to genetic variations generated by natural selection in response to diverse environmental challenges. Further investigate the biological roles of the identified motifs, especially those not associated with known domains (motifs 2, 3, 9, and 10) that could determine their potential interactions with other proteins or nucleic acids to elucidate their functional significance. However, PPIs analysis of NO-induced *NBS-LRR* proteins in Arabidopsis through the STRING database revealed physical associations with related disease-related proteins in the network, indicating strong interactions that underscore their role in plant defense against pathogens. The results also documented CHS1, known for its disease-resistance properties, also indicated its role in conferring cold stress resistance by mitigating chloroplast damage and cell death, signifying the multi-layered nature of the studied genes.

Subsequently, our aim was to investigate how post-translational modification, especially S-Nitrosylation which involves the attachment of a NO group to cysteine residues, can influence the functioning of crucial proteins within plant immune signaling pathways [39, 58]. Accurately identifying S-Nitrosylated substrates and their specific sites is essential for elucidating the intricate molecular mechanisms leading S-Nitrosylation. Therefore, we used GPS-SNO 1.0 software to predict the S-Nitrosylation sites in the studied *NBS-LRR* genes of *A. thaliana*, *O. sativa*, *Z. mays*, *G. max*, *and S. lycopersicum* (Fig. 5; Supplementary Table 5). We have identified a significant number of S-nitrosylation sites within their protein sequences. This discovery offers valuable insights into the regulatory role of NO at the protein level in the respective species, as well as their post-translational modifications in response to pathogen attacks. However, it is important to mention that although homologous proteins have similar sequences, we found some differences in their 3D folding structures (Supplementary

Fig. 1–5). However, though homologous proteins share a common evolutionary origin and often have similar sequences, variations in their amino acid sequences can lead to differences in their three-dimensional structures. These structural differences may result in variations in their functions, even though they may still perform related roles within the cell. This phenomenon is generally called divergent evolution, where proteins evolve different structures and functions from a common ancestor. It is a fascinating area of study because it highlights the versatility and adaptability of the *NBS-LRR* proteins in response to different evolutionary pressures. Furthermore, the fold changes of both qRT-PCR and RNA-Seq results dignify their participants in the plant's defense mechanisms. The comprehensive bioinformatic analyses conducted on the NBS-LRR genes have provided valuable insights into the molecular mechanisms underlying plant immunity.

Conclusions

This study comprehensively analyzed 29 NO-induced *NBS-LRR* gene of *A. thaliana* including twenty-seven *NBS-LRR* genes of *O. sativa*, *Z. mays*, *G. max*, *and S. lycopersicum*. Physio-chemical characterization of these genes provides detailed information about their position, structure, and roles, which is crucial for understanding their function in protein formation. The selected *NBS-LRR* genes have light, hormonal, stress and growth responsive *cis*-elements in their promoter region. Additionally, numerous S-Nitrosylation sites were identified, suggesting NO's regulatory role and post-translational modifications in response to pathogens that might be prone to future challenges discovering the molecular functions. In a nutshell, the pathogen-responsive *NBS-LRR* genes identified in this study hold promise as candidate genes for engineering pathogen resistance in the respective species.

Materials and methods

NBS-LRR sequence extraction and characterization

Hussain, et al. [59] conducted a comprehensive analysis of the *A. thaliana* leaf transcriptome in response to nitric oxide and elucidated distinct molecular pathways that regulate plant responses to abiotic and biotic stresses. Using three replicates each of control and 1mM S-nitrosocysteine (CysNO)-infiltrated Arabidopsis accession Col-0 leaf samples at the rosette stage, they sequenced 84 to 91 million reads, resulting in the identification of 32,535 genes and 55,682 transcripts. Following this, we identified twenty-nine (29) nitric oxide-induced *NBS-LRR* transcripts from the transcriptomic dataset and retrieved their respective genomic information and sequences from the TAIR database (https://www.Arabidopsis.org/, accessed on 06 December 2023). Furthermore, the NBS-LRR related genes and their genomic data from rice (*Oryza sativa*), maize (*Zea mays*), soybean (*Glycine max*), and tomato (*Solanum lycopersicum*) were collected from the respective databases; Rice Genome Annotation Project (http://rice.uga.edu/), Gramene (https://www.gramene.org/), Soybase (https://www.soybase.org/), and Phytozome 13 (https://phytozome-next.jgi.doe.gov/), respectively (Accessed on 06 December 2023). Gene sequences were mined using "NBS-LRR" as a keyword and via BLAST. Subsequently, motifs were identified via https://www.genome.jp/tools/motif/, (accessed on 06 December 2023) to verify the presence of the NBS-LRR motif in the identified sequences for further analysis. Various physicochemical properties of the retrieved protein sequences, such as the Protein Molecular Weight (kDa), theoretical isoelectric point (pI), and grand average of hydropathicity (GRAVY) were determined using the ExPASy database (https://web.expasy.org/protparam/ accessed on 07 December 2023). CELLO v.2.5: subCELlular Localization predictor (http://cello.life.nctu.edu.tw/ accessed on 07 December 2023) was used to predict the subcellular localization of *NBS-LRR* proteins based on significant reliability.

Phylogenetic tree and conserved domains

Phylogenetic analysis was performed for the *NBS-LRR* genes of *A. thaliana*, *O. sativa*, *Z. mays*, *G. max*, and *S. lycopersicum*. Sequences were aligned via multiple sequence alignments (MSA) using the MUSCLE algorithm within the MEGA X 10.1.8 program [60, 61]. Next, we employed the Maximum Likelihood method to build phylogenetic trees with 1000 bootstrap replicates to assess the robustness of the tree topology [62]. The analysis was based on mRNA sequences, ensuring a more accurate representation of the evolutionary relationships among the *NBS-LRR* genes of the various plant species under study. This approach enhances the reliability of the phylogenetic inference, providing valuable insights into the evolutionary divergence and relationships of *NBS-LRR* genes across these plant species. We further characterized the protein sequences by identifying the domain type and precise positions of the *NBS-LRR* domains. This analysis was conducted using the NCBI Conserved Domain Database (https://www.ncbi.nlm.nih.gov/Structure/cdd/wrpsb.cgi) (accessed on 08 December 2023) [63]. To enhance the interpretation of the results, we employed TBtools-II v2.102 [64], a bio-sequence structure illustrator, for visualizing the identified domains.

Analysis of gene structure, cis-regulatory elements, and conserved motifs

The Gene Structure Display Server 2.0 [65] (accessed on 22 December 2023) was used to elucidate the gene structure of NBS-LRRs genes [65]. Furthermore, for

each *NBS-LRR* gene in *A. thaliana*, *O. sativa*, *Z. mays*, *G. max*, and *S. lycopersicum*, a 1000-base pair nucleotide sequence (Up-stream of the start codon) of the 5`UTR was extracted. These sequences were subsequently utilized as query sequences in the PlantCARE database [66] (accessed on 22 December 2023) for the identification of potential *cis*-regulatory elements, finally combined according to their role in the hormonal, stress, and developmental responses. To find the conserved motifs in the *NBS-LRR* proteins, Multiple EM for motif elicitation (MEME) (accessed on 22 December 2023) was utilized [67]. The maximum number of motifs was selected as 10, and the other parameters were left as default.

Protein-protein interaction and prediction of S-nitrosylation site

To explore protein-protein interactions (PPIs) among the 56 *NBS-LRR* related proteins identified in *A. thaliana*, *O. sativa*, *Z. mays*, *G. max*, and *S. lycopersicum*, an in-silico PPI network was predicted using the STRING v.12 (accessed on 28 December 2023), a web tool for Protein-Protein Interaction Networks analysis [68]. Besides, we used GPS-SNO 1.0 software to predict and identify cysteine residues that could be the target of NO-based modification via S-Nitrosylation [69]. GPS-SNO 1.0 has demonstrated its efficiency and speed in predicting S-Nitrosylation sites, achieving an accuracy of 75.80%, a specificity of 53.57%, and a sensitivity of 80.14%. AlphaFold protein structure files were downloaded from the protein database as PDB files and imported to the protein visualization and analysis software Pymol 2.5.5 [70] where they were further analyzed.

CIRCOS plot and gene expression patterns

CIRCOS plot was drawn using TBtools [64] to show a summary of the previous transcriptomic data set with special emphasis on the *A. thaliana* 29 *NBS-LRR* genes, their location, before and after-treatment FPKM values, and changes in expression via an integrated heatmap. Real-time quantitative PCR was performed for selected *NBS-LRR* genes as described by Hussain et al. [59]. Primer sequences can be found in Supplementary Table 6. PCR reactions were performed with three biological replicates with actin (*ACT2*), and a no-template control reaction was used as internal comparative controls. The qRT-PCR results were statistically compared with the transcriptomic data that displayed in Supplementary Table 7.

Supplementary Information

The online version contains supplementary material available at https://doi.org/10.1186/s12870-024-05587-3.

Supplementary Material 1

Supplementary Material 2

Supplementary Material 3

Supplementary Material 4

Supplementary Material 5

Supplementary Material 6

Supplementary Material 7

Supplementary Material 8

Supplementary Material 9

Supplementary Material 10

Supplementary Material 11

Supplementary Material 12

Acknowledgements

This research was supported by Basic Science Research Program through the National Research Foundation of Korea (NRF) funded by the Ministry of Education (RS-2023-00245922). Quantitative PCR was done at KNU NGS center (Daegu, South Korea). We thankful to the Global Korea Scholarship (GKS) of the Government of Republic of Korea for funding post-graduate student.

Author contributions

Conceptualization, investigation, data analysis and writing original draft, A.K.D.; conceptualization, data analysis, validation, review and editing, A.H.; investigation, N.J.M., D.-S.L., G.-J.L. and Y.-J.W.; project administration and funding acquisition, B.-W.Y. All authors have reviewed and approved the final version of the manuscript.

Funding

This research was supported by the Korea Basic Science Institute (National Research Facilities and Equipment Center) grant funded by the Ministry of Education (2021R1A6C101A416).

Data availability

All data is included within the manuscript and supplementary tables. Additional information can be provided by the corresponding author upon request.

Declarations

Ethics approval and consent to participate

Not applicable.

Consent for publication

Not applicable.

Competing interests

The authors declare no competing interests.

Received: 31 May 2024 / Accepted: 12 September 2024
Published online: 09 October 2024

References

1. Jones JD, Dangl JL. The plant immune system. Nature. 2006;444(7117):323–9.
2. Kourelis J, Van Der Hoorn RA. Defended to the nines: 25 years of resistance gene cloning identifies nine mechanisms for R protein function. Plant Cell. 2018;30(2):285–99.
3. Qian L-H, Wang Y, Chen M, Liu J, Lu R-S, Zou X, Sun X-Q, Zhang Y-M. Genome-wide identification and evolutionary analysis of NBS-LRR genes from Secale cereale. Front Genet. 2021;12:771814.
4. Meyers BC, Dickerman AW, Michelmore RW, Sivaramakrishnan S, Sobral BW, Young ND. Plant disease resistance genes encode members of an ancient

and diverse protein family within the nucleotide-binding superfamily. Plant J. 1999;20(3):317–32.
5. Martin GB, Bogdanove AJ, Sessa G. Understanding the functions of plant disease resistance proteins. Annu Rev Plant Biol. 2003;54(1):23–61.
6. Meyers BC, Kozik A, Griego A, Kuang H, Michelmore RW. Genome-wide analysis of NBS-LRR–encoding genes in Arabidopsis. Plant Cell. 2003;15(4):809–34.
7. McDowell JM, Woffenden BJ. Plant disease resistance genes: recent insights and potential applications. Trends Biotechnol. 2003;21(4):178–83.
8. Xiao S, Emerson B, Ratanasut K, Patrick E, O'Neill C, Bancroft I, Turner JG. Origin and maintenance of a broad-spectrum disease resistance locus in Arabidopsis. Mol Biol Evol. 2004;21(9):1661–72.
9. Collier SM, Hamel L-P, Moffett P. Cell death mediated by the N-terminal domains of a unique and highly conserved class of NB-LRR protein. Mol Plant-Microbe Interact. 2011;24(8):918–31.
10. Shao Z-Q, Zhang Y-M, Hang Y-Y, Xue J-Y, Zhou G-C, Wu P, Wu X-Y, Wu X-Z, Wang Q, Wang B. Long-term evolution of nucleotide-binding site-leucine-rich repeat genes: understanding gained from and beyond the legume family. Plant Physiol. 2014;166(1):217–34.
11. Wang T, Jia Z-H, Zhang J-Y, Liu M, Guo Z-R, Wang G. Identification and analysis of NBS-LRR genes in Actinidia chinensis genome. Plants. 2020;9(10):1350.
12. Yu X, Zhong S, Yang H, Chen C, Chen W, Yang H, Guan J, Fu P, Tan F, Ren T. Identification and characterization of NBS resistance genes in Akebia trifoliata. Front Plant Sci. 2021;12:758559.
13. Sagi MS, Deokar AA, Tar'an B. Genetic analysis of NBS-LRR gene family in chickpea and their expression profiles in response to Ascochyta blight infection. Front Plant Sci. 2017;8:838.
14. Yin T, Han P, Xi D, Yu W, Zhu L, Du C, Yang N, Liu X, Zhang H. Genome-wide identification, characterization, and expression profile of NBS-LRR gene family in sweet orange (Citrus sinensis). Gene. 2023;854:147117.
15. Zhang W, Yuan Q, Wu Y, Zhang J, Nie J. Genome-wide identification and characterization of the CC-NBS-LRR gene family in cucumber (Cucumis sativus l). Int J Mol Sci. 2022;23(9):5048.
16. Wang J, Yang C, Wu X, Wang Y, Wang B, Wu X, Lu Z, Li G. Genome-wide characterization of NBS-LRR family genes and expression analysis under powdery mildew stress in Lagenaria siceraria. Physiol Mol Plant Pathol. 2022;118:101798.
17. Zhang Y-M, Chen M, Sun L, Wang Y, Yin J, Liu J, Sun X-Q, Hang Y-Y. Genome-wide identification and evolutionary analysis of NBS-LRR genes from Dioscorea rotundata. Front Genet. 2020;11:484.
18. Kohler A, Rinaldi C, Duplessis S, Baucher M, Geelen D, Duchaussoy F, Meyers BC, Boerjan W, Martin F. Genome-wide identification of NBS resistance genes in Populus trichocarpa. Plant Mol Biol. 2008;66:619–36.
19. Andersen EJ, Nepal MP, Purintun JM, Nelson D, Mermigka G, Sarris PF. Wheat disease resistance genes and their diversification through integrated domain fusions. Front Genet. 2020;11:898.
20. Goyal N, Bhatia G, Sharma S, Garewal N, Upadhyay A, Upadhyay SK, Singh K. Genome-wide characterization revealed role of NBS-LRR genes during powdery mildew infection in Vitis vinifera. Genomics. 2020;112(1):312–22.
21. Li X, Zhang Y, Yin L, Lu J. Overexpression of pathogen-induced grapevine TIR-NB-LRR gene VaRGA1 enhances disease resistance and drought and salt tolerance in Nicotiana Benthamiana. Protoplasma. 2017;254:957–69.
22. Xun H, Yang X, He H, Wang M, Guo P, Wang Y, Pang J, Dong Y, Feng X, Wang S. Over-expression of GmKR3, a TIR–NBS–LRR type R gene, confers resistance to multiple viruses in soybean. Plant Mol Biol. 2019;99:95–111.
23. Li NY, ma XF, Short DP, Li TG, Zhou L, Gui YJ, Kong ZQ, Zhang DD, Zhang WQ, Li JJ. The island cotton NBS-LRR gene GbaNA1 confers resistance to the non-race 1 verticillium dahliae isolate Vd991. Mol Plant Pathol. 2018;19(6):1466–79.
24. Betz WJ, Mao F, Smith CB. Imaging exocytosis and endocytosis. Curr Opin Neurobiol. 1996;6(3):365–71.
25. Ryan TA, Smith SJ, Reuter H. The timing of synaptic vesicle endocytosis. *Proceedings of the National Academy of Sciences* 1996, 93(11):5567–5571.
26. Delledonne M, Xia Y, Dixon RA, Lamb C. Nitric oxide functions as a signal in plant disease resistance. Nature. 1998;394(6693):585–8.
27. Durner J, Wendehenne D, Klessig DF. Defense gene induction in tobacco by nitric oxide, cyclic GMP, and cyclic ADP-ribose. *Proceedings of the National Academy of Sciences* 1998, 95(17):10328–10333.
28. Wang Y-Q, Feechan A, Yun B-W, Shafiei R, Hofmann A, Taylor P, Xue P, Yang F-Q, Xie Z-S, Pallas JA. S-nitrosylation of AtSABP3 antagonizes the expression of plant immunity. J Biol Chem. 2009;284(4):2131–7.
29. Romero-Puertas MC, Campostrini N, Mattè A, Righetti PG, Perazzolli M, Zolla L, Roepstorff P, Delledonne M. Proteomic analysis of S-nitrosylated proteins in Arabidopsis thaliana undergoing hypersensitive response. Proteomics. 2008;8(7):1459–69.
30. Lawrence SR, Gaitens M, Guan Q, Dufresne C, Chen S. S-nitroso-proteome revealed in stomatal guard cell response to flg22. Int J Mol Sci. 2020;21(5):1688.
31. Ali R, Ma W, Lemtiri-Chlieh F, Tsaltas D, Leng Q, von Bodman S, Berkowitz GA. Death don't have no mercy and neither does calcium: Arabidopsis CYCLIC NUCLEOTIDE GATED CHANNEL2 and innate immunity. Plant Cell. 2007;19(3):1081–95.
32. Machchhu F, Wany A. Protein S-nitrosylation in plants under biotic stress. Theoretical Experimental Plant Physiol 2023;35:331–339.
33. Wilkinson JQ, Crawford NM. Identification of the Arabidopsis CHL3 gene as the nitrate reductase structural gene NIA2. Plant Cell. 1991;3(5):461–71.
34. Hao L, Yu C, Li B, Wang D. Molecular cloning and preliminary analysis of TaNOA in common wheat. Sheng Wu Gong Cheng Xue bao = Chin J Biotechnol. 2010;26(1):48–56.
35. Vitor SC, Duarte GT, Saviani EE, Vincentz MG, Oliveira HC, Salgado I. Nitrate reductase is required for the transcriptional modulation and bactericidal activity of nitric oxide during the defense response of Arabidopsis thaliana against Pseudomonas syringae. Planta. 2013;238:475–86.
36. Hussain A, Imran QM, Shahid M, Yun B-W. Nitric oxide synthase in the plant kingdom. In: *Nitric Oxide in Plant Biology.* Edited by Pratap Singh V, Singh S, Tripathi DK, Romero-Puertas MC, Sandalio LM: Academic Press; 2022: 43–52.
37. Modolo LV, Augusto O, Almeida IM, Pinto-Maglio CA, Oliveira HC, Seligman K, Salgado I. Decreased arginine and nitrite levels in nitrate reductase-deficient Arabidopsis thaliana plants impair nitric oxide synthesis and the hypersensitive response to Pseudomonas syringae. Plant Sci. 2006;171(1):34–40.
38. Malik SI, Hussain A, Yun B-W, Spoel SH, Loake GJ. GSNOR-mediated de-nitrosylation in the plant defence response. Plant Sci. 2011;181(5):540–4.
39. Yun B-W, Feechan A, Yin M, Saidi NB, Le Bihan T, Yu M, Moore JW, Kang J-G, Kwon E, Spoel SH. S-nitrosylation of NADPH oxidase regulates cell death in plant immunity. Nature. 2011;478(7368):264–8.
40. Borrowman S, Kapuganti JG, Loake GJ. Expanding roles for S-nitrosylation in the regulation of plant immunity. Free Radic Biol Med. 2023;194:357–68.
41. Kwon E, Feechan A, Yun BW, Hwang BH, Pallas JA, Kang JG, Loake GJ. AtGSNOR1 function is required for multiple developmental programs in Arabidopsis. Planta. 2012;236(3):887–900.
42. Hussain A, Yun B-W, Kim JH, Gupta KJ, Hyung N-I, Loake GJ. Novel and conserved functions of S-nitrosoglutathione reductase in tomato. J Exp Bot. 2019;70(18):4877–86.
43. Jia Y, Yuan Y, Zhang Y, Yang S, Zhang X. Extreme expansion of NBS-encoding genes in Rosaceae. BMC Genet. 2015;16:1–12.
44. DeYoung BJ, Innes RW. Plant NBS-LRR proteins in pathogen sensing and host defense. Nat Immunol. 2006;7(12):1243–9.
45. Delledonne M, Zeier J, Marocco A, Lamb C. Signal interactions between nitric oxide and reactive oxygen intermediates in the plant hypersensitive disease resistance response. Proc Natl Acad Sci. 2001;98(23):13454–9.
46. Delledonne M, Xia Y, Dixon R, Lorenzoni C, Lamb C. Nitric oxide signalling in the plant hypersensitive disease resistance response. In: *Genetics and Breeding for Crop Quality and Resistance: Proceedings of the XV EUCARPIA Congress, Viterbo, Italy, September 20–25, 1998: 1999*. Springer: 127–133.
47. Sánchez-Martín J, Steuernagel B, Ghosh S, Herren G, Hurni S, Adamski N, Vrána J, Kubaláková M, Krattinger SG, Wicker T. Rapid gene isolation in barley and wheat by mutant chromosome sequencing. Genome Biol. 2016;17:1–7.
48. Witek K, Jupe F, Witek AI, Baker D, Clark MD, Jones JD. Accelerated cloning of a potato late blight–resistance gene using RenSeq and SMRT sequencing. Nat Biotechnol. 2016;34(6):656–60.
49. Liu Y, Du H, Li P, Shen Y, Peng H, Liu S, Zhou G-A, Zhang H, Liu Z, Shi M. Pan-genome of wild and cultivated soybeans. Cell. 2020;182(1):162–76. e113.
50. Poland J, Rutkoski J. Advances and challenges in genomic selection for disease resistance. Annu Rev Phytopathol. 2016;54:79–98.
51. Ameline-Torregrosa C, Wang B-B, O'Bleness MS, Deshpande S, Zhu H, Roe B, Young ND, Cannon SB. Identification and characterization of nucleotide-binding site-leucine-rich repeat genes in the model plant Medicago truncatula. Plant Physiol. 2008;146(1):5–21.
52. Liu Y, Li D, Yang N, Zhu X, Han K, Gu R, Bai J, Wang A, Zhang Y. Genome-wide identification and analysis of CC-NBS-LRR family in response to downy mildew and black rot in Chinese cabbage. Int J Mol Sci. 2021;22(8):4266.
53. Frazier TP, Palmer NA, Xie F, Tobias CM, Donze-Reiner TJ, Bombarely A, Childs KL, Shu S, Jenkins JW, Schmutz J. Identification, characterization, and gene expression analysis of nucleotide binding site (NB)-type resistance gene homologues in switchgrass. BMC Genomics. 2016;17:1–17.

54. Martin R, Qi T, Zhang H, Liu F, King M, Toth C, Nogales E, Staskawicz BJ. Structure of the activated ROQ1 resistosome directly recognizing the pathogen effector XopQ. Science. 2020;370(6521):eabd9993.
55. Roy SW, Gilbert W. Rates of intron loss and gain: implications for early eukaryotic evolution. Proc Natl Acad Sci. 2005;102(16):5773–8.
56. Long M, VanKuren NW, Chen S, Vibranovski MD. New gene evolution: little did we know. Annu Rev Genet. 2013;47:307–33.
57. Xu G, Guo C, Shan H, Kong H. Divergence of duplicate genes in exon–intron structure. Proc Natl Acad Sci. 2012;109(4):1187–92.
58. Pande A, Mun B-G, Khan M, Rahim W, Lee D-S, Lee G-M, Al Azawi TNI, Hussain A, Yun B-W. Nitric oxide signaling and its association with ubiquitin-mediated proteasomal degradation in plants. Int J Mol Sci. 2022;23(3):1657.
59. Hussain A, Mun B-G, Imran QM, Lee S-U, Adamu TA, Shahid M, Kim K-M, Yun B-W. Nitric oxide mediated transcriptome profiling reveals activation of multiple regulatory pathways in Arabidopsis thaliana. Front Plant Sci. 2016;7:975.
60. Edgar RC. MUSCLE: a multiple sequence alignment method with reduced time and space complexity. BMC Bioinformatics. 2004;5:1–19.
61. Kumar S, Stecher G, Li M, Knyaz C, Tamura K. MEGA X: molecular evolutionary genetics analysis across computing platforms. Mol Biol Evol. 2018;35(6):1547–9.
62. Felsenstein J. Confidence limits on phylogenies: an approach using the bootstrap. Evolution. 1985;39(4):783–91.
63. Wang J, Chitsaz F, Derbyshire MK, Gonzales NR, Gwadz M, Lu S, Marchler GH, Song JS, Thanki N, Yamashita RA. The conserved domain database in 2023. Nucleic Acids Res. 2023;51(D1):D384–8.
64. Chen C, Wu Y, Li J, Wang X, Zeng Z, Xu J, Liu Y, Feng J, Chen H, He Y. TBtools-II: a one for all, all for one bioinformatics platform for biological big-data mining. Mol Plant. 2023;16(11):1733–42.
65. Hu B, Jin J, Guo A-Y, Zhang H, Luo J, Gao G. GSDS 2.0: an upgraded gene feature visualization server. Bioinformatics. 2015;31(8):1296–7.
66. Lescot M, Déhais P, Thijs G, Marchal K, Moreau Y, Van de Peer Y, Rouzé P, Rombauts S. PlantCARE, a database of plant cis-acting regulatory elements and a portal to tools for in silico analysis of promoter sequences. Nucleic Acids Res. 2002;30(1):325–7.
67. Bailey TL, Johnson J, Grant CE, Noble WS. The MEME suite. Nucleic Acids Res. 2015;43(W1):W39–49.
68. Szklarczyk D, Kirsch R, Koutrouli M, Nastou K, Mehryary F, Hachilif R, Gable AL, Fang T, Doncheva NT, Pyysalo S. The STRING database in 2023: protein–protein association networks and functional enrichment analyses for any sequenced genome of interest. Nucleic Acids Res. 2023;51(D1):D638–46.
69. Xue Y, Liu Z, Gao X, Jin C, Wen L, Yao X, Ren J. GPS-SNO: computational prediction of protein S-nitrosylation sites with a modified GPS algorithm. PLoS ONE. 2010;5(6):e11290.
70. DeLano WL. Pymol: an open-source molecular graphics tool. CCP4 Newsl Protein Crystallogr. 2002;40(1):82–92.

Publisher's note